View metadata, citation and similar papers at core.ac.uk

brought to you by CORE

provided by VCU Scholars Compass

Virginia Commonwealth University
VCU Scholars Compass

Chemistry Publications

Dept. of Chemistry

2006

Reversible paramagnetism to ferromagnetism in transition metal-doped TiO2 nanocrystals prepared by microwave irradiation

Garry Glaspell
Virginia Commonwealth University

Asit B. Panda
Virginia Commonwealth University

M. S. El-Shall
Virginia Commonwealth University, mselshal@vcu.edu

Follow this and additional works at: http://scholarscompass.vcu.edu/chem_pubs

Part of the Chemistry Commons

Glaspell, G., Panda, A. B., & El-Shall, M. S. Reversible paramagnetism to ferromagnetism in transition metal-doped TiO2 nanocrystals prepared by microwave irradiation. Journal of Applied Physics, 100, 124307 (2006). Copyright © 2006 American Institute of Physics.

Downloaded from

http://scholarscompass.vcu.edu/chem_pubs/18

This Article is brought to you for free and open access by the Dept. of Chemistry at VCU Scholars Compass. It has been accepted for inclusion in Chemistry Publications by an authorized administrator of VCU Scholars Compass. For more information, please contact libcompass@vcu.edu.

Reversible paramagnetism to ferromagnetism in transition metal-doped TiO_2 nanocrystals prepared by microwave irradiation

Garry Glaspell, Asit B. Panda, and M. S. El-Shall[a)]
Department of Chemistry, Virginia Commonwealth University, Richmond, Virginia 21284-2006

(Received 21 December 2005; accepted 4 October 2006; published online 21 December 2006)

TiO_2 nanoparticles doped with 1%, 5%, and 10% M (M=Co, Fe, and Ni) were prepared by microwave irradiation and characterized using x-ray diffraction, transmission electron microscopy, and magnetometry. The as-prepared samples are found to be paramagnetic at room temperature, with the magnetic susceptibility following the Curie-Weiss law in the investigated range of 2–300 K. However, transformation from paramagnetism to room-temperature ferromagnetism (RTFM) was observed by hydrogenating the samples at 400 °C. Reheating in air converted the samples back to paramagnetic while rehydrogenating the samples again induced ferromagnetism. It is argued that the reversible RTFM observed is due to interaction between the dopant metal ions and oxygen vacancies produced during hydrogenation. X-ray diffraction of the hydrogenated Co- and Fe-doped samples shows only a single TiO_2 phase suggesting that the observed RTFM may be intrinsic, but for the Ni-doped samples the magnetism may arise from metallic Ni on the surfaces of the TiO_2 nanoparticles. © *2006 American Institute of Physics*. [DOI: 10.1063/1.2400805]

I. INTRODUCTION

The design, synthesis, and characterization of dilute magnetic semiconductors (DMSs) have recently attracted considerable attention.[1–3] These materials represent ideal systems for spin-based semiconductor devices which are expected to offer improved performance, lower power consumption, and higher speeds than the conventional charge-based systems.[1–3] Among different semiconductor hosts that have been investigated for DMS applications, the transition metal-doped TiO_2 materials have been the subject of intense research since the report of room-temperature ferromagnetism (RTFM) of the Co-doped TiO_2 thin films by Matsumoto *et al.*[4] Although a large number of Co-doped TiO_2 systems have been studied, the origin of RTFM has not yet been clearly established.[5–22] The major question of the controversy is whether the ferromagnetic coupling results from the presence of segregated Co clusters because of the high Curie temperature of bulk Co ($T_C \approx 1388$ K) (Refs. 8 and 10) or from the substitution of Co^{2+} ions for the Ti^{4+} ions which results in the exchange coupling between the Co ions through the charge carriers induced by oxygen defects.[4,5] Clearly, the preparation conditions, the distribution and concentration of the Co ions, and the microstructures of the doped TiO_2 materials will influence the observed magnetic properties.[5–22]

In a recent study, Manivannan *et al.* have prepared 10% Co/TiO_2 (mainly anatase) powder by a sol-gel technique and found it to be paramagnetic (PM) in the 2–370 K range.[16,23] However, by heating the sample to 400 °C in a H_2/Ar mixture part of the PM sample was converted into RTFM, and by reheating the sample at 300 °C in air, the sample was converted back to PM.[23] The reversible nature of the PM to FM state was taken as evidence that the observed RTFM in the hydrogenated sample is due to CO^{2+} exchange interaction mediated by the oxygen vacancies produced by hydrogenation.[9,23] Since the sample preparation by the sol-gel technique and the nature and distribution of the dopant can alter the PM to FM reversibility, it is important to investigate these effects in samples prepared by alternative methods.

Herein, we report the preparation of transition metal (M)-doped TiO_2 nanoparticles (M=Co, Fe, and Ni) using a simple approach based on the microwave synthesis of nanoparticles from metal salts in solutions. Microwave irradiation (MWI) has several advantages over conventional solution synthesis methods since selective dielectric heating, due to the difference in the solvent and reactant dielectric constants, can provide significant enhancement in reaction rates which results in short reaction time, small particle size, narrow size distribution, and high purity.[24–30] Furthermore, MWI methods are unique in providing scaled-up processes without suffering thermal gradient effects, thus leading to a potentially industrially important advancement in the large-scale synthesis of DMS nanomaterials.

II. EXPERIMENT

Synthesis of the transition metal-doped doped TiO_2 nanoparticles was achieved following the preparation of titanium hydroxide by the hydrolysis of titanium isopropoxide in a water-alcohol mixture under basic conditions. The precipitate of $TiO_2 \cdot n(H_2O)$ was filtered and washed extensively. The required amount of hydrous titanium oxide was then slowly dissolved in dilute nitric acid with continuous stirring for 30 min at room temperature, resulting in a clear solution of aqueous titanium nitrate. The appropriate amount of aqueous $Co(NO_3)_2$, $Fe(NO_3)_3$, or $Ni(NO_3)_2$ solution was then added with continuous stirring. Dropwise addition of dilute ammonia to this solution up to pH 12 resulted in the formation of metal hydroxide solution with highly dispersed

[a)]Electronic mail: selshall@hsc.vcu.edu

 © 2006 American Institute of Physics

[This article is copyrighted as indicated in the article. Reuse of AIP content is subject to the terms at: http://scitation.aip.org/termsconditions. Downloaded to] IP: 128.172.48.59 On: Fri, 06 Nov 2015 17:47:38

metal ions. Immediately after hydroxide formation, dilute nitric acid was added to the solution to make the *p*H of the solution ~5 and the solution was immediately transferred to a conventional microwave oven and irradiated for 30 min. The microwave power was set to 33% of 650 W and operated in 30 s cycles (on for 10 s off 20 s) for 30 min. After irradiation, the *p*H of the solution was again adjusted to 12 by the addition of ammonium hydroxide and the solution was reirradiated. The microwave reirradiation under basic *p*H conditions ensures that no free metal ions remain in the solution. After drying, parts of the resulting powders were used for magnetic measurements and the remaining parts were used for the hydrogenation treatment carried out at 673 K. The hydrogen reduction setup consisted of a tube furnace with a gas flow control unit. The sample contained in an open glass boat and placed inside the tubule furnace where a 5% H_2/Ar gas mixture was passed over the sample for 4 h at 673 K. All reagents were purchased from Aldrich Chemical Co. and used without further purification.

The x-ray diffraction (XRD) patterns of the powder samples were measured at room temperature with an X'Pert Philips Materials Research diffractometer, with Cu Kα_1 radiation. The samples were mounted on a silicon plate for x-ray measurements. Transmission electron microscopy (TEM) was carried out using a JEOL JEM-1230 electron microscope operated at 120 kV. Temperature (T) and magnetic field (H) variations of the magnetization (M) of the as-prepared and treated samples were measured using a commercial superconducting quantum interference device magnetometer (SQUID, Quantum Design).

III. RESULTS AND DISCUSSION

Figure 1(a) displays the XRD patterns of the 10% Co-doped TiO_2 sample under different conditions according to (i) as prepared, (ii) after hydrogenation at 673 K, (iii) after heating in air at 673 K following the hydrogenation step, and (iv) after rehydrogenation at 673 K. It is evident that the XRD patterns match well with that of the anatase phase of TiO_2 (Ref. 31) with a trace amount of the brookite phase[32] also present. However, no evidence of peaks corresponding to the Co dopant is found, indicating that the Co is well dispersed throughout the TiO_2 lattice. It is important to note that the Co peaks are not observed even after repeated cycles of heating in a H_2/Ar mixture and in air at 673 K. The volume-weighted average crystalline size calculated from the XRD peak width using Scherrer's equation[33] indicates that the average TiO_2 particle size is ~7 nm. This value agrees well with the TEM images of the as-prepared and the hydrogenated samples shown in Figs. 1(b) and 1(c), respectively.

Figure 2(a) (top) shows the temperature dependence of the magnetic susceptibility $\chi = M/H$ for the as-prepared 10% Co/TiO_2 (prior to hydrogenation). The paramagnetic nature of the sample is evident from the excellent fit of χ to the Curie-Weiss law: $\chi = \chi_0 + C/(T-\theta)$, with $\theta = -0.9$ K. This dependence is similar to the one reported for 10% Co/TiO_2 prepared using a sol-gel synthesis.[16,23] From the Curie constant $C = 1.7 \times 10^{-3}$ emu K/gOe ($C = N\mu^2/3k_B$, with N being the number of magnetic ions/g, k_B Boltzmann constant, and

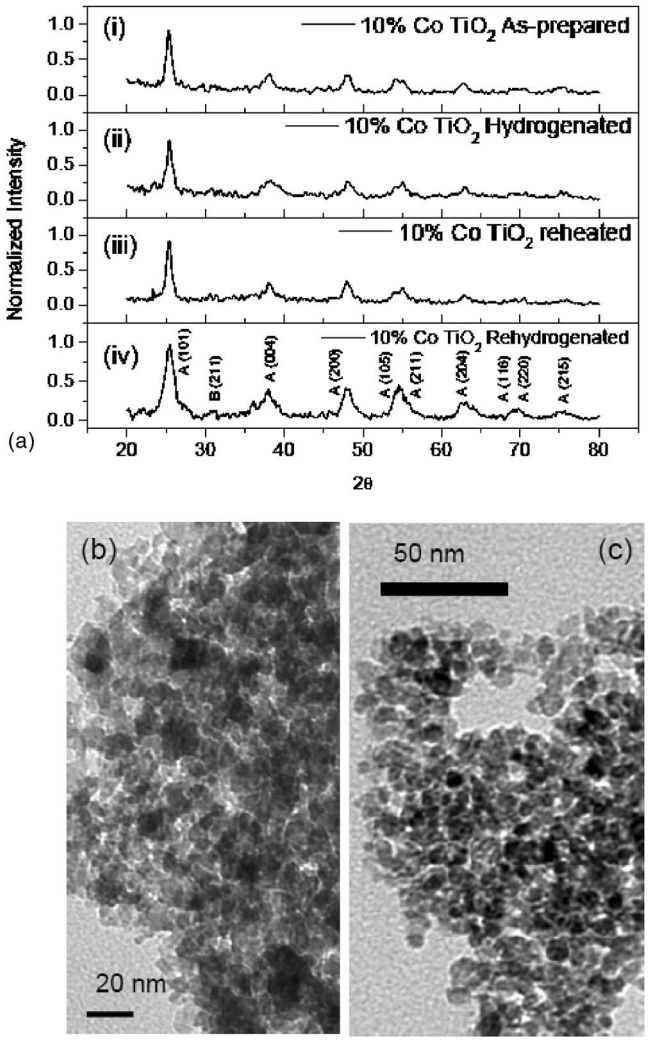

FIG. 1. (a) XRD patterns for 10% Co/TiO_2: (i) as prepared, (ii) hydrogenated, (iii) reheated in air, and (iv) rehydrogenated. For the assignment of XRD, A=anatase and B=brookite. (b) TEM micrograph of the as-prepared 10% Co/TiO_2 nanoparticles. (c) TEM micrograph of 10% Co/TiO_2 nanoparticles after hydrogenation.

μ magnetic moment), $\mu(Co^{2+}) = 3.3\mu_B$ is obtained. This magnitude of μ is somewhat smaller than the value of 4.1 obtained for the 10% Co/TiO_2 prepared using the sol-gel procedure.[16] However, the assumption is still that Co^{2+} substitutes for Ti^{4+} in the anatase unit cell with the balance of the charge compensated for by the surrounding oxygen. After hydrogenation at 400 °C for 4 h, the sample is transformed into a ferromagnetic as indicated by the temperature dependence of χ measured under zero-field-cooled (ZFC) and field-cooled (FC) conditions, as shown in Fig. 2(a) (bottom). However, this ferromagnetic behavior cannot be attributed to the presence of Co nanoparticles in our sample since no peak was observed in χ for the ZFC case. Observation of a peak in χ under ZFC conditions is considered a signature of the blocking temperature (T_B) for cobalt, as reported for the thin films of Co/TiO_2.[12]

The M vs H variations for the as-prepared 10% Co/TiO_2 sample prior to and after hydrogenation are shown in Fig. 2(b). The linear variation of M vs H for the as-prepared sample is indicative of paramagnetism while the hydrogen-

[This article is copyrighted as indicated in the article. Reuse of AIP content is subject to the terms at: http://scitation.aip.org/termsconditions. Downloaded to] IP: 128.172.48.59 On: Fri, 06 Nov 2015 17:47:38

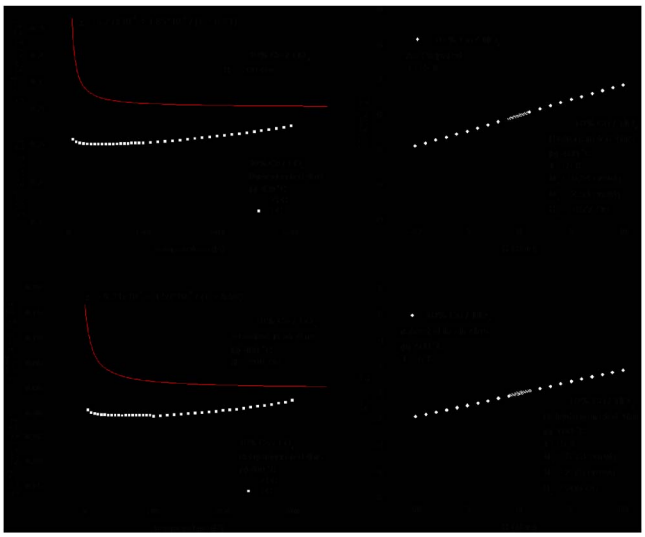

FIG. 2. (Color online) Temperature dependence of the magnetic susceptibility (χ) for 10% Co/TiO_2: [(a), top] as prepared, [(a) bottom] after hydrogenation under field-cooled (FC) and zero-field-cooled (ZFC) conditions. (b) M vs H variations measured at 5 K for the as-prepared and hydrogenated 10% Co/TiO_2 samples. [(c) top] Temperature dependence of the magnetic susceptibility (χ) for 10% Co/TiO_2 reheated in air and rehydrogenated [(c) bottom] under FC and ZFC conditions. (d) M vs H variations measured at 5 K for the reheated in air and rehydrogenated 10% Co/TiO_2 samples.

ated sample shows full hysteresis loops from 5 to 300 K. The remanence M_r (M at $H=0$) and coercivity H_c (H at $M=0$) measured at 5 K were 2.53 emu/g and 1077 Oe, respectively as shown in Table I. Hysteresis loops were also observed at 300 K with a remanence and coercivity of 1.98 emu/g and 381 Oe, respectively, as shown in Table I. It is significant to note that at both 5 and 300 K, the coercivity is more than double the values obtained for the 10% Co/TiO_2 samples prepared by the sol-gel technique.[16] The average magnetic size can be determined from the slope of the magnetization near zero field with the major contributions arising from the largest particles. Using Eq. (1) below,[34] where k is the Boltzmann constant, T is the temperature, dM/dH is the slope near zero field, M_s is the saturation magnetization, and ρ is the bulk density of Co, an upper bound for the magnetic size can be estimated, as shown in Table I.

$$d_{\max} = \left[\frac{10kT}{\pi} \frac{(dM/dH)}{\rho M_s^2} \right]^{1/3}. \quad (1)$$

The small value of the magnetic size (~3 nm, smaller than the actual TiO_2 nanoparticles as determined from the TEM data) also indicates that the Co is well dispersed in the TiO_2 sample, thus confirming the uniform mixing during the microwave irradiation.

Reheating the sample in air (400 °C) transforms the observed ferromagnetism back to its original paramagnetic character. It is significant to note that the sample again follows the Curie-Weiss behavior, and the Curie constant after reheating is similar to that observed in the as-prepared sample, as shown in Fig. 2(c). Also, $\mu(Co^{2+})=3.3\mu_B$ for the reheated sample is similar to the corresponding value of the as-prepared sample, which indicates that hydrogenation does not affect the state of the Co in the TiO_2 lattice. This ultimately supports the claim that the observed RTFM arises from the produced oxygen vacancies. The linear M vs H observed for the reheated sample in air, and the hysteresis loops measured after rehydrogenation, shown in Fig. 2(d), confirm the reversibility of the PM to FM transition in the 10% Co/TiO_2 sample. The coercivity and remanence observed at both 5 and 300 K after rehydrogenation are similar to the values obtained from the first hydrogenation, as shown in Table I.

The temperature variation of the coercivity H_c of the 10% Co/TiO_2 sample after the first hydrogenation indicates a critical temperature T_c (the temperature at which spontaneous magnetization vanishes) of approximately 435 K. This value is close to the T_c obtained for the rehydrogenated sample (488 K) which indicates that the state of Co remains unaffected within the TiO_2 lattice after repeated cycles of hydrogenation. The T_c obtained for the rehydrogenated sample is similar to the T_c determined for the hydrogenated 10% Co/TiO_2 prepared via the sol-gel process ($T_c \approx 470$ K).[16]

We have also measured the magnetic properties of 2.5% Co/TiO_2 and 5% Co/TiO_2 samples prepared by MWI to see if controlled PM to FM transformations are possible with different doping levels. The 2.5% Co/TiO_2 sample followed the Curie-Weiss behaviors both for the as-prepared and after hydrogenation, indicating that at such small doping level, not enough Co^{2+} exists within TiO_2 lattice to induce FM after hydrogenation. However, hydrogenation of the 5% Co/TiO_2 sample resulted in the transformation to RTFM. It is significant to note that the observed coercivities at both 5 and 300 K of 5% Co/TiO_2 sample are similar to the values de-

TABLE I. Temperature variations of the remanence (M_r) and the coercivity (H_c) data of Co- and Fe-doped TiO_2 nanoparticles after hydrogenation for 4 h at 400 °C.

Sample	M_r (emu/g)	H_c (Oe)	M_s (emu/g)	Magnetic size (nm)	Critical temp (K)
5% Co/TiO_2 hydrogenated				4.7	466
$T=5$ K	0.87	1170	1.94		
$T=300$ K	0.68	368	1.66		
10% Co/TiO_2 hydrogenated				3.2	435
$T=5$ K	2.53	1077	6.54		
$T=300$ K	1.98	381	5.00		
10% Co/TiO_2 rehydrogenated				3.2	488
$T=5$ K	2.75	905	6.73		
$T=300$ K	1.95	378	5.39		
10% Fe/TiO_2 hydrogenated				3.1	1074
$T=5$ K	0.25	325	3.66		
$T=300$ K	0.16	268	2.06		
10% Fe/TiO_2 rehydrogenated				4.3	952
$T=5$ K	0.19	272	3.08		
$T=300$ K	0.013	231	1.86		

[This article is copyrighted as indicated in the article. Reuse of AIP content is subject to the terms at: http://scitation.aip.org/termsconditions. Downloaded to] IP: 128.172.48.59 On: Fri, 06 Nov 2015 17:47:38

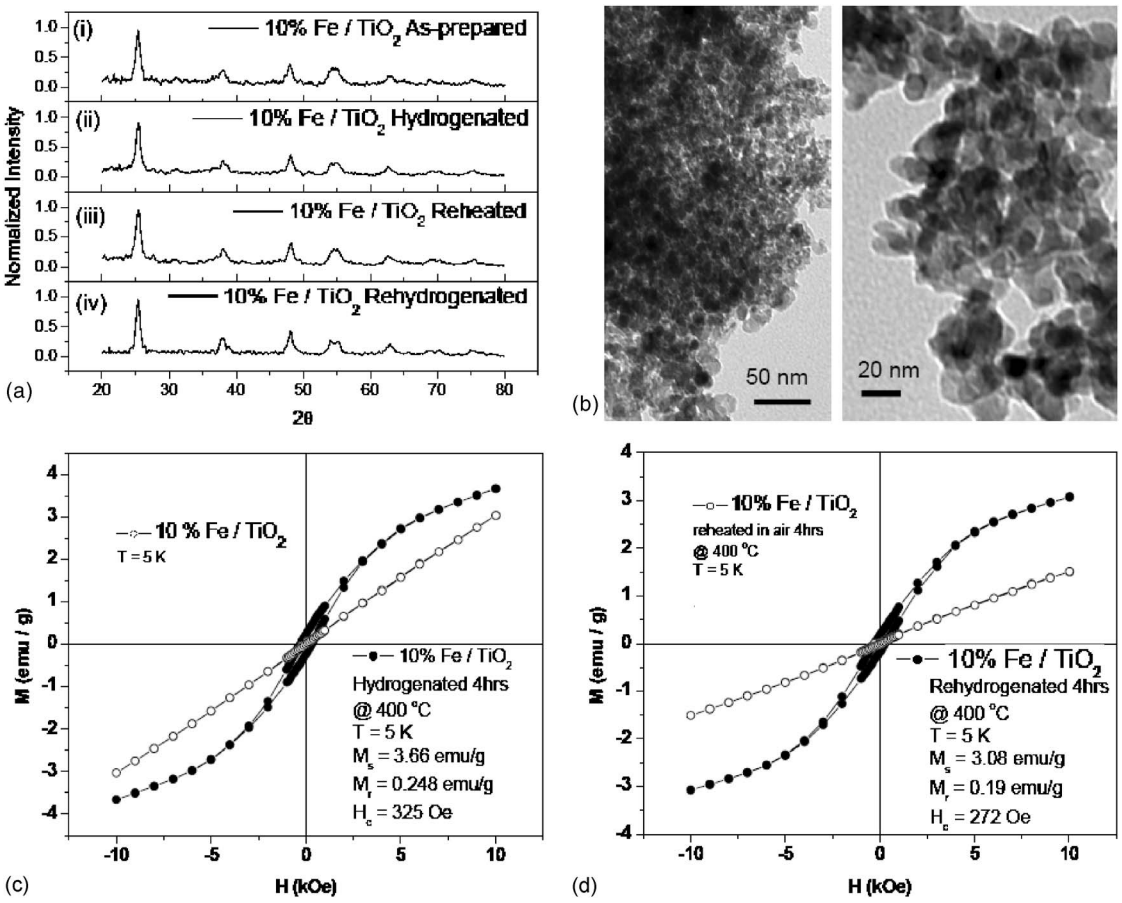

FIG. 3. (a) XRD patterns for 10% Fe/TiO_2: (i) as-prepared, (ii) hydrogenated, (iii) reheated in air, and (iv) rehydrogenated. (b) TEM micrographs of the as-prepared 10% Fe/TiO_2 nanoparticles (left) and after hydrogenation (right). (c) M vs H variations measured at 5 K for the as-prepared and hydrogenated 10% Fe/TiO_2 samples. (d) M vs H variations measured at 5 K for the reheated in air and rehydrogenated 10% Fe/TiO_2 samples.

termined for the 10% doped sample. This result suggests that the ratios of Co^{2+} to the oxygen vacancies are similar for both the 5% and 10% doped samples, which implies that Co^{2+} may prefer to reside inside the TiO_2 nanoparticles rather than on the surface. Also, the critical temperature calculated for the 5% doped sample (466 K) is close to that of the 10% doped sample (435 K) providing further evidence that the state of Co is the same in both samples. Table I lists the remanence M_r, the coercivity H_c, the saturation magnetization M_s, the magnetic size domain, and the critical temperature T_c determined for the samples prepared by MWI.

Similar reversible behavior was observed for the Fe-doped TiO_2 system. Figure 3(a) displays the XRD patterns of the 10% Fe-doped TiO_2 sample (i) as prepared, (ii) after hydrogenation at 673 K, (iii) after heating in air at 673 K following the hydrogenation step, and (iv) after rehydrogenation at 673 K. Similar to the Co-doped system, no XRD peaks corresponding to the dopant are present, indicating that the Fe is well dispersed throughout the TiO_2 lattice. The TEM images of the as-prepared and the hydrogenated samples, shown in Fig. 3(b), indicate that the samples consist of nanocrystals with an average size of 5–7 nm. Hydrogenation converts the sample from paramagnetic to a ferromagnetic. The linear M vs H variation shows hysteresis after hydrogenation as shown in Fig. 3(c) with the relevant values reported in Table I. While reheating the sample in air again converts the sample back to paramagnetic which displays a linear M vs H variation at 5 K, as shown in Fig. 3(d), the sample does not exhibit a pronounced deviation between the FC and ZFC cases as observed in the Co-doped system. This result indicates that the state of Fe may change during hydrogenation of the 10% Fe-doped TiO_2 sample. However, this change is not evident in the XRD data shown in Fig. 3(a). On the other hand, the data shown in Table I indicate a significant increase in the magnetic size domain and a decrease in the critical temperature of the 10% Fe-doped TiO_2 sample after the rehydrogenation cycle. Therefore, the change in the state of Fe during hydrogenation cannot be ruled out from the current data.

For the Co- and Fe-doped systems it appears that the Co and Fe are well dispersed throughout the titania lattice. However, for the Ni-doped TiO_2 system, we observe a different scenario. The reversible PM to FM behavior was observed even for the 2.5% Ni-doped TiO_2 sample after hydrogenation. As the Ni concentration increases to 10%, the critical temperature also increases consistent with increasing the amount of Ni on the surfaces of the TiO_2 nanoparticles. The XRD pattern of the as-prepared 10% Ni-doped TiO_2, shown in Fig. 4(a), matches well with the anatase pattern with no observed peaks corresponding to Ni. The temperature dependence of χ for the as-prepared 10% Ni-doped sample also follows the Curie-Weiss behavior with a calculated $\mu(Ni^{2+})$

[This article is copyrighted as indicated in the article. Reuse of AIP content is subject to the terms at: http://scitation.aip.org/termsconditions. Downloaded to] IP: 128.172.48.59 On: Fri, 06 Nov 2015 17:47:38

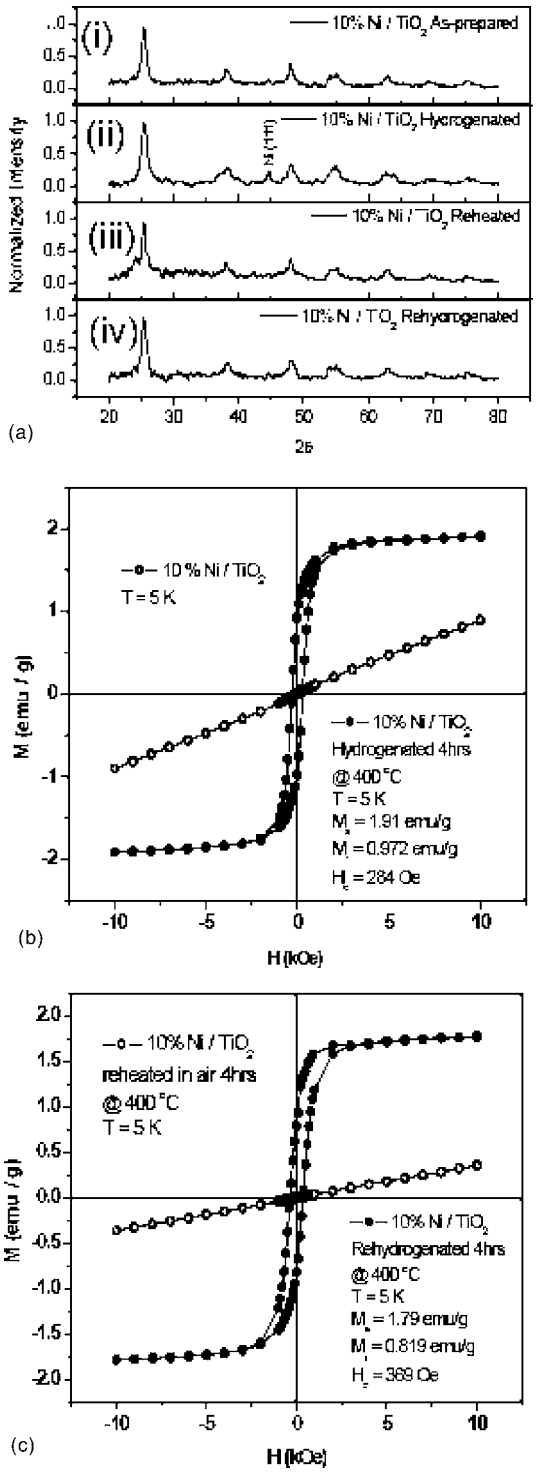

FIG. 4. (a) XRD patterns for 10% Ni/TiO_2: (i) as-prepared, (ii) hydrogenated, (iii) reheated in air, and (iv) rehydrogenated. (b) M vs H variations measured at 5 K for the as-prepared and hydrogenated 10% Ni/TiO_2 samples. (c) M vs H variations measured at 5 K for the reheated in air and rehydrogenated 10% Ni/TiO_2 samples.

$=1.8\mu_B$ somewhat lower than the accepted value of 3.2.[35] Hydrogenation converts the sample from paramagnetic to ferromagnetic with observed hysteresis loops, as shown in Fig. 4(b). However, the XRD pattern of the hydrogenated sample indicates the presence of metallic Ni, as shown in Fig. 4(a) (ii). Reheating the hydrogenated sample in air converts the sample back to paramagnetic which again displays the Curie-Weiss behavior similar to the as-prepared sample. Rehydrogenation again induces RTFM although the XRD pattern after rehydrogenation does not show the characteristic diffraction from the (111) plane of Ni observed in the first hydrogenation treatment. The observation of the (111) diffraction peak from Ni in the XRD pattern of the first hydrogenation treatment may suggest that the observed RTFM of the 10% Ni-doped TiO_2 could be induced by metallic Ni present within the TiO_2 nanoparticles. However, it is not clear why the metallic Ni is not observed in the XRD pattern of the repeated hydrogenated sample. It is clear that further studies are needed in order to conclusively establish the origin of the RTFM in the Ni-doped TiO_2 nanoparticles.

IV. CONCLUSIONS

In conclusion, we have demonstrated the synthesis of transition metal-doped TiO_2 nanoparticles via microwave irradiation. The significance of the current method lies mainly in its simplicity, flexibility, short reaction times, high purity, high yield, and the control of the different factors that determine the magnetic properties of the doped titania. The XRD data of the Co-and Fe-doped TiO_2 show the formation of the anatase phase without any indication of the presence of metallic dopants. While it is generally accepted that XRD does not detect small quantities ($<2\%$), we believe that the absence of a blocking temperature and the small domain size calculated for the Co- and Fe-doped samples, even at 10% loading, provides strong evidence that the metals are well dispersed within the titania lattice. We have shown that the as-prepared samples are paramagnetic, hydrogenating the samples transform the samples to ferromagnetic, and that this phenomenon is reversible. Theoretically, it has been suggested that oxygen vacancies are essential to provide the exchange coupling between the doped ions leading to RTFM; thus, the hydrogenation experiments are likely to extract oxygen from the titania lattice producing oxygen vacancies which may account for the reversibility of the RTFM.

ACKNOWLEDGMENT

Acknowledgment is made to the Donors of the American Chemical Society Petroleum Research Fund No. PRF41602-AEF.

[1]H. Ohno, Science **281**, 951 (1998).
[2]J. D. Bryan, S. M. Heald, S. A. Chambers, and D. R. Gamelin, J. Am. Chem. Soc. **126**, 11640 (2004).
[3]R. Janisch, P. Gopal, and N. A. Spaldin, J. Phys.: Condens. Matter **17**, R657 (2005).
[4]Y. Matsumoto *et al.*, Science **291**, 854 (2001).
[5]S. A. Chambers *et al.*, Appl. Phys. Lett. **79**, 3467 (2001).
[6]Y. Matsumoto *et al.*, Jpn. J. Appl. Phys., Part 2 **40**, L1205 (2001).
[7]W. K. Park, R. J. Ortega-Hertogs, J. Moodera, A. Punnoose, and M. S. Seehra, J. Appl. Phys. **91**, 8093 (2002).
[8]D. H. Kim, Appl. Phys. Lett. **81**, 2421 (2002).
[9]M. S. Park, S. K. Kwon, and B. I. Min, Phys. Rev. B **65**, 161201 (2002).
[10]J. Y. Kim, Phys. Rev. Lett. **90**, 017401 (2003).
[11]P. A. Stampe, R. J. Kennedy, Y. Xin, and J. S. Parker, J. Appl. Phys. **93**, 7864 (2003).
[12]A. Punnoose, M. S. Seehra, W. K. Park, and J. S. Moodera, J. Appl. Phys. **93**, 7867 (2003).
[13]D. H. Kim *et al.*, J. Appl. Phys. **93**, 6125 (2003).
[14]B. Z. Rameev, F. Yildiz, L. R. Tagirov, B. Aktas, W. K. Park, and J. S.

[This article is copyrighted as indicated in the article. Reuse of AIP content is subject to the terms at: http://scitation.aip.org/termsconditions. Downloaded to] IP: 128.172.48.59 On: Fri, 06 Nov 2015 17:47:38

Moodera, J. Magn. Magn. Mater. **258–259**, 361 (2003).
[15]A. Manivannan, M. S. Seehra, S. B. Majumder, and R. S. Katiyar, Appl. Phys. Lett. **83**, 111 (2003).
[16]A. Manivannan, G. Glaspell, and M. S. Seehra, J. Appl. Phys. **94**, 6994 (2003).
[17]V. Shutthanandan *et al.*, Appl. Phys. Lett. **84**, 4466 (2004).
[18]H. Toyosaki, T. Fukumura, Y. Yamada, K. Nakajima, T. Chikyow, T. Hasegawa, H. Koinuma, and M. Kawasaki, Nature (London) **3**, 221 (2004).
[19]H. Yang and R. Singh, J. Appl. Phys. **95**, 7192 (2004).
[20]N. Hong, W. Prellier, J. Sakai, and A. Ruyter, J. Appl. Phys. **95**, 7378 (2004).
[21]R. Kennedy, P. Stampe, E. Hu, P. Xion, S. von Molar, and Y. Xin, Appl. Phys. Lett. **84**, 2832 (2004).
[22]M. Cui, J. Zhu, X. Zhong, Y. Zhao, and X. Duan, Appl. Phys. Lett. **85**, 1698 (2004).
[23]A. Manivannan, G. Glaspell, and M. S. Seehra, J. Appl. Phys. **97**, 10D325 (2005).
[24]O. Palchik, J. Zhu, and A. Gedankan, J. Mater. Chem. **10**, 1251 (2000).
[25]J. Zhu, O. Palchik, S. Chen, and A. Gedanken, J. Phys. Chem. B **104**, 7344 (2000).
[26]D. Boxall and C. Lukehart, Chem. Mater. **13**, 806 (2001).
[27]K. Gallis and C. Landry, Adv. Mater. (Weinheim, Ger.) **13**, 23 (2001).
[28]J. Liang, Z. X. Deng, X. Jiang, F. Li, and Y. Li, Inorg. Chem. **41**, 3602 (2002).
[29]G. Glaspell, L. Fuoco, and M. S. El-Shall, J. Phys. Chem. B **109**, 17350 (2005).
[30]A. B. Panda, G. Glaspell, and M. S. El-Shall, J. Am. Chem. Soc. **128**, 2790 (2006).
[31]ICCD Report No. 01-078-2486 (unpublished).
[32]ICCD Report No. 01-075-1582 (unpublished).
[33]H. P. Klug and L. E. Alexander, *X-ray Diffraction Procedures for Polycrystalline and Amorphous Materials* 2nd ed. (Wiley, New York, 1974).
[34]I. I. Yaacob, A. C. Nunes, A. Bose, and D. O. Shah, J. Colloid Interface Sci. **168**, 289 (1994).
[35]C. Kittel, *Introduction to Solid State Physics* (Wiley, New York, 1986).

[This article is copyrighted as indicated in the article. Reuse of AIP content is subject to the terms at: http://scitation.aip.org/termsconditions. Downloaded to] IP: 128.172.48.59 On: Fri, 06 Nov 2015 17:47:38